LIGHTWEIGHT STRUCTURES in CIVIL ENGINEERING
CONTEMPORARY PROBLEMS
Monograph from Scientific Seminar
Organized by Polish Chapters of
International Association for Shell and Spatial Structures
Łódź University of Technology
Faculty of Civil Engineering, Architecture
and Environmental Engineering
XXVII LSCE
Łódź, 2nd – 3rd of December 2021

The impact of footing conditions of a vertical-axis floating-roof tank on structural shell deformation

K. Żyliński [1] **J. Górski** [2]
[1] Faculty of Civil and Environmental Engineering, Gdańsk University of Technology POLAND
Rodoverken, Poland; zylinskikamil@gmail.com
[2] Faculty of Civil and Environmental Engineering, Gdańsk University of Technology, POLAND
jgorski@pg.edu.pl

ABSTRACT: Structural shells of fuel tanks are often subjected to geometric imperfections which may lead to exceeding the ultimate and serviceability limit states. One of the means triggering shell deformation is non-uniform settlement caused by incoherent soil conditions. Analysis carried out in the work concerns of vertical-axis, floating-roof cylindrical shell which volume is 50.000 m^3, founded on a complex multi-layered soil. The sensitivity analysis was conducted of a tank settlement due to variation of material soil parameters and the strata layout. It reads that even in the case of extremely disadvantageous material data the structure is not bound to exceed the serviceability limit states.

Keywords: storage tanks, foundation settlement, subsoil parameters, sensitivity analysis.

1. INTRODUCTION

Fuel tank design should be considered as a highest-standard task due to possible environmental pollution in case of possible structural failure. The FE models are bound to exceed the standards of deterministic analysis of perfect structures, to consider the issues of geometric and material imperfections, post-welding stresses [Rasiulis et al. 2006] etc. Reliability analysis may be employed to assess structural degradation due to corrosion [Geary & Hobbs 2013]. In selected cases footing conditions should be regarded while they may lead to limit state exceedance [Grget et al. 2018, Gunerathne et al. 2018, Ignatowicz & Hotala 2020, Nassernia & Showkati 2020]. The attempts of structural optimization are denoted too [Magnucki et al. 2006]. The paper analyses the fuel tank of a vertical axis, with a floating roof. Scope of calculation is restricted to the estimation of the impact of diverse soil conditions to the tank shell deformation. The impact of geometric and material imperfections is neglected, the interaction of tank footing is investigated only. Non-uniform settlement may produce excessive tank deformation and stress increase, subsequently, operational obstacles e.g. by floating roof locking. The in-situ experimental results make it possible to realistically reflect complex soil conditions. The computations are limited to sensitivity analysis of the tank shell to the variation of foundation conditions. The work incorporates the procedures addressed in [Żyliński et al. 2021, 2020].

2. OUTLOOK ON A FUEL TANK WITH A FLOATING ROOF

The work analyses a vertical-axis cylindrical fuel tank (Fig. 1) of a 50000 m^3 volume, designed according to the EN 14015 standard (hoop stress criterion). The shell stability due to extreme wind pressure according to the standard EN 1993-4-1 and considering local action was checked numerically in the light of EN 1993-1-6. Wind cover shell was also designed in the case of failure and leakage of the stored medium. This additional structural element was not considered in the computations. The design assumes the S355J2 steel for the structure. The tank diameter is 60.5 m, its height is 22.0 m. Fig. 1 presents the tank model and the information on sheet thicknesses in meters. All the computations were performed in the ZSoil environment [Commend et. al] combined with Python aided modules.

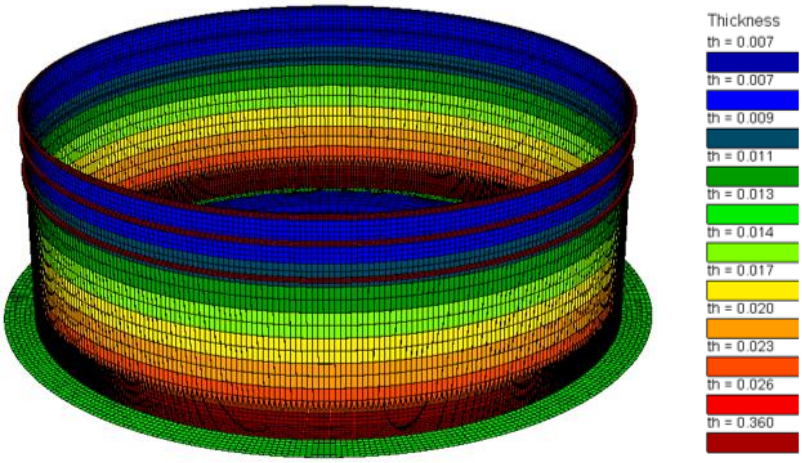

Fig. 1. The tank overview, regarding variable shell thickness (ZSoil)

In addition, Table 1 shows the sheet thicknesses due to standards, t_{ini}, and the effective ones, reduced by corrosion, t_{efect}. Table 1 also presents the data on heights of distinct courses and their location.

Table 1. The heights and thicknesses of distinct sections of the tank

No.	t_{init} [mm]	t_{efect} [mm]	h [m]	$h_{overall}$ [m]
9	11	7,5	2,25	2,25
8	11	7,5	2,25	4,50
7	12	8,5	2,25	6,75
6	15	11,4	2,50	9,25
5	18	14,4	2,50	11,75
4	21	17,4	2,50	14,25
3	24	20,4	2,50	16,75
2	27	23,2	2,50	19,25
1	30	26,2	2,75	22,00

The numerical model incorporates the reduced sheet thicknesses t_{efect}, hence the computations reflect the structure in its occupation. Moreover, reducing the structural stiffness made an indirect impact of some means: initial imperfections, sheet fabrication tolerances, post-welding stresses and other means which are hard to detect. The wind cover plates thicknesses were not included in Table 1. while this structural part was not analyzed. Second shell weight was assumed in the form of a nodal load of 12.04 kN. The mean Young's modulus E = 210 GPa and the mean Poisson's ratio ν = 0.3 were taken for the analysis. The corner ring was

designed in the form of a panel 0.36 m thick to reflect the minimum stiffness required by the standard EN 14015, it was fixed 0.25 m below the shell top edge.
The sub-foundation region was discretized by eight-node 3D elements whose parameters represent the structural parts, i.e.: ring foundation, sand ballast and relevant soil strata. The foundation strip was modelled as a RC element whose dimensions are 4.05×3.0 m (Fig. 2).
The transfer of friction forces between the sheet, the soil and the concrete foundation strip was considered by the so-called contact introduced to the model. The functions are applied corresponding to the friction coefficients based on the PN-82/B-02003 standard, i.e.: $\mu = 0.3$.
The soil regions of the footing subjected to sensitivity analysis are presented in Fig. 2b in orange, green and pink. The elements marked in yellow between the strip and the external area correspond to the soil parameters in the tank vicinity $E = 128$ MPa. The stiffness modulus of concrete mixed with sand (marked in greenish) is denoted by a value $E = 130$ MPa, because this is not the concrete made on the building site by mixing cement with aggregate.

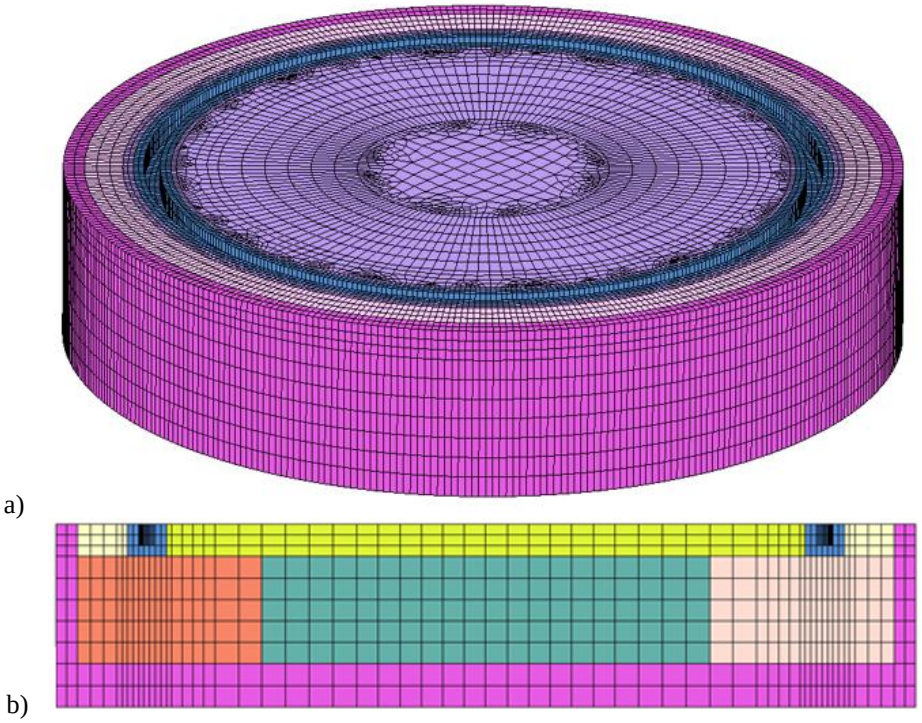

Fig. 2. Three-dimensional overview of a tank a) foundation section, b) subsoil section

The boundary elements of the subsoil (marked in violet, Fig. 2) form a layer whose effective Young's modulus is $E = 50$ MPa. The numerical values are bound to consider the deformation impact of an infinite zone. The reduced stiffness of the elements surrounding the computational domain allows to minimize the boundary conditions effect by non-controlled vertical deformation caused by fixed horizontal edges of adjacent elements.
The soil strata layout based on the drillings are displayed in Fig. 3, their parameters are collected in Table 2. Due to Young's moduli diversity the area beneath the tank is divided into five regions of variable stiffness, marked *KZ*. The sensitivity analysis incorporates elastic subsoil model employing mean Young's moduli of each region, included in Table 2.
According to the design the tank is filled in with a liquid up to the level of 19.6 m from the bottom, yielding operational hydrostatic pressure. The computations also consider uniform pressure on the tank bottom corresponding to the liquid pressure of the height 19.6 m. The medium density equals 1000 kg/m3. With regard to the roof structure the variable load (snow) does not occur in this case. The analysis also neglects

the wind load because its interaction with the liquid pressure on the walls is remote, not resulting in considerable actions on the foundation.

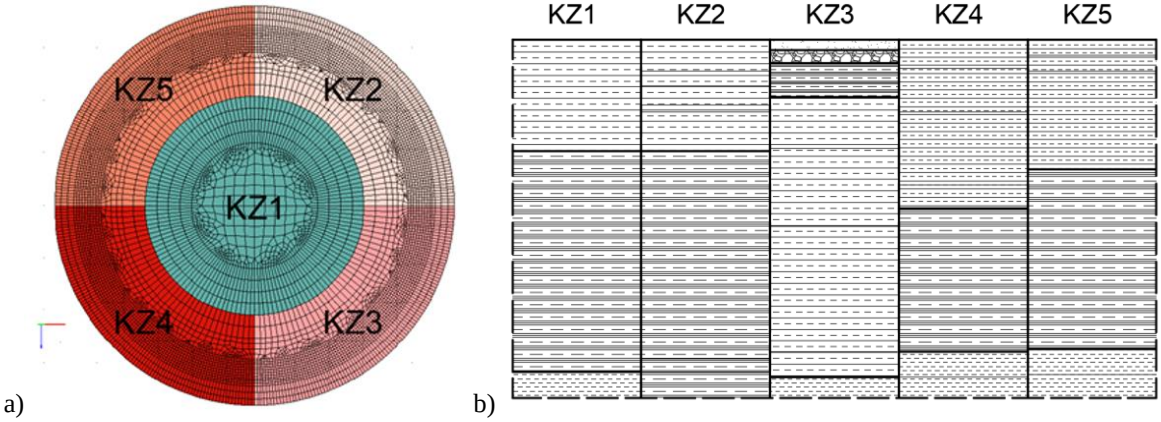

a) b)

Fig. 3 Distributions: a) subsoil strata, b) five distinct material parameters

Table 2. Material parameters of subsoil strata (measurement results at selected boreholes)

*KZ*1		*KZ*2		*KZ*3		*KZ*4		*KZ*5	
t [m]	*E* [kPa]	*T* [m]	*E* [kPa]	*t*[m]	*E* [kPa]	*t* [m]	*E* [kPa]	*t* [m]	*E* [kPa]
4.3	30.88	1.2	14.6	0.4	62.97	1.1	14.59	0.6	14.59
8.5	46.31	0.6	30.7	0.5	144.59	1.7	24.28	0.6	24.28
1	24.47	0.7	19.6	0.4	14.59	2.8	30.88	3.8	30.88
0	24.47	0.3	24.3	0.3	30.65	0.9	39.91	6.9	46.31
-	-	1.5	30.7	0.6	39.91	5.5	46.31	1	24.47
-	-	8	46.3	2.0	30.65	1	24.47	0	24.47
-	-	0.5	39.9	3.0	39.91	0	24.47	-	-
-	-	0	39.9	4.8	46.31	-	-	-	-
-	-	-	-	1.0	24.47	-	-	-	-
-	-	-	-	0.0	24.47	-	-	-	-
E_{mean} [kPa]	39.92	38.54		43.40		35.30		37.57	
σ_{KZ} [kPa]	10.30	10.94		37.22		10.74		10.59	
μ_{KZi} [-]	0.26	0.28		0.86		0.30		0.28	

3. SENSITIVITY ANALYSIS

Analysis of the settlement impact on the shape deformation and the tank effort requires appropriate computational models. It is a highly important task while the impact of various footing conditions is compared. The comparative analysis employs two means, i.e.: extreme vertical deformations of the bottom and vertical bending moments causing additional shell deformation.

Variation of mechanical response of a structure is investigated to the variation of foundation parameters. The subsoil is modelled in two variants.

The first approach distinguishes five subregions *KZ*1-*KZ*5 on the basis of the Table 2, these regions are marked with appropriate Young's moduli. The model in Fig. 3a yields deformation of the bottom central node equal $u_5 = 0.066$ m (5 is a number of distinctly assumed material parameters). While the parameters *KZ* of all regions are averaged to a single value *KZ* = 38.95 kPa the maximum settlement of the bottom raises up to $u1 = 0.069$ m. This difference is slight because all the material parameters *KZ*1-*KZ*5 are close to their

mean value KZ = 38.95 kPa. Tab. 3 presents the deformation of the annular plate. They yield a conclusion that no threat of limit state exceedance occurs here.

Table 3. The results - perimeter sheet of a tank

	u_y [m]	σ_{ya} [m]	min(u_y) [m]	max(u_y) [m]
5 *KZ*	-0.01891	0.00428	-0.02809	-0.01353
1 *KZ*	-0.01877	0.00428	-0.02731	-0.01398

The next step addresses the impact of stiffness modulus *KZ* variation of selected regions according to Tab. 4. The test is aimed at determining the relationship type between the stiffness variation and the anticipated mechanical response of the tank.

Table 4 The input data - sensitivity analysis - model II

No.	E_{mean} [MPa]	Sensitivity analysis [MPa]			
		E_{mean} (1+0.1σ)	E_{mean} (1+0.4 σ)	E_{mean} (1-0.1 σ)	E_{mean} (1-0.4 σ)
*KZ*1	42,71	46,99	59,80	38,44	25,63
*KZ*2	37,19	40,91	52,07	33,47	22,32
*KZ*3	41,23	45,36	57,73	37,11	24,74
*KZ*4	38,12	41,93	53,37	34,31	22,87
*KZ*5	39,98	43,97	55,97	35,98	23,99

The relation between the assumed moduli and the results is presented in Table 5 and Fig. 4. The results regarding perimeter sheet deformation may be approximated linearly while variation of bottom stiffness is non-linear (Fig. 4).

Table 5. The results - settlements, variable Young's modulus of the input data - model II

		Annular plate				Bottom
		u_y [m]	σ_{ya} [m]	min(u_y) [m]	max(u_y) [m]	u_{yd} [m]
II	KZ(n) +0,1v	-0,0176	0,0041	-0,0263	-0,0126	-0,0619
	KZ(n) +0,4v	-0,0148	0,0036	-0,0226	-0,0100	-0,0532
	KZ(n) -0,1v	-0,0205	0,0045	-0,0302	-0,0147	-0,0710
	KZ(n) -0,4v	-0,0286	0,0057	-0,0407	-0,0207	-0,0958

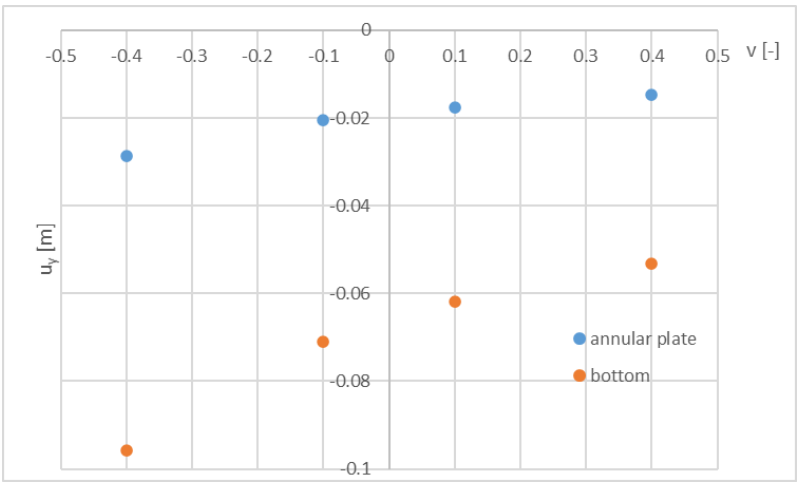

Fig. 4. The relationship - deflections vs variable subsoil stiffness

The last analytical step of structural response to variable subsoil conditions assumes each KZ parameter change independent (Fig. 3), according to Fig. 5.

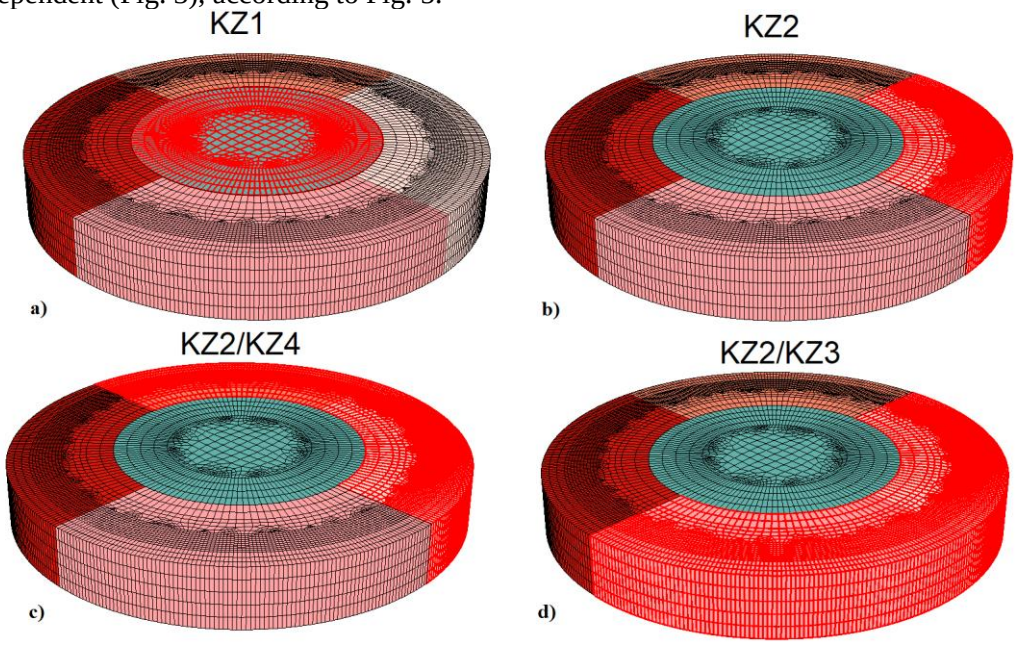

Fig. 5. Distinction of subregions in the models of sensitivity analysis

While the parameter KZ1 varies (Fig. 5a) the stiffness is reduced to reach the extreme bottom settlement. The second regarded model (Fig. 5b) concerns the variations in structural strains due to overstiffening or weakening of KZ2. Such a configuration of subsoil parameters may trigger local foundation ring settlement, subsequently, irregular deformations of a boundary sheet and the bottom part. Two latter cases are aimed at selective reduction of subsoil stiffness, bringing irregular and extreme variations in sheet stresses and deflections. A featured important parameter in tank operation is the variation of radial deflection of the stiffening ring, at the elevation of the tank head. The results are included in Table 6. Most cases are grouped in pairs (Tab. 6)

Table 6. The input data - sensitivity analysis - model III

No.	KZ1 [MPa]	KZ2 [MPa]	KZ3 [MPa]	KZ4 [MPa]
KZ1 -0.3 E_{mean}	29.90	-	-	-
KZ2 -0.3 E_{mean}	-	26.03	-	-
KZ2 -0.5 E_{mean}	-	18.60	-	-
KZ2/4 +0.3 E_{mean}	-	48.35	-	49.56
KZ2/4 -0.3 E_{mean}	-	26.03	-	26.69
KZ2/4 -0.5 E_{mean}	-	18.60	-	19.06
KZ2/4 -0.8 E_{mean}	-	7.44	-	7.76
KZ2/3 -0.3 E_{mean}	-	26.03	28.86	-
KZ2/3 -0.5 E_{mean}	-	18.60	20.62	-
KZ2/3 -0.8 E_{mean}	-	7.44	8.25	-

Global deformation of the shell and the subsoil is presented in Fig. 6, the results are collected in Table 7. The analysis of bottom and boundary (perimeter) sheet deflections (Fig. 6) yields that the extreme reduction of the central region stiffness a local, point deflection difference occurs, up to u = 0.224 m. Such a point difference is irrational hence the form of subsoil parameter introduction should be verified. Other differences

in average deflections remain constant at the level of u = 0.07 m in the case of parameter variation of boundary layers.

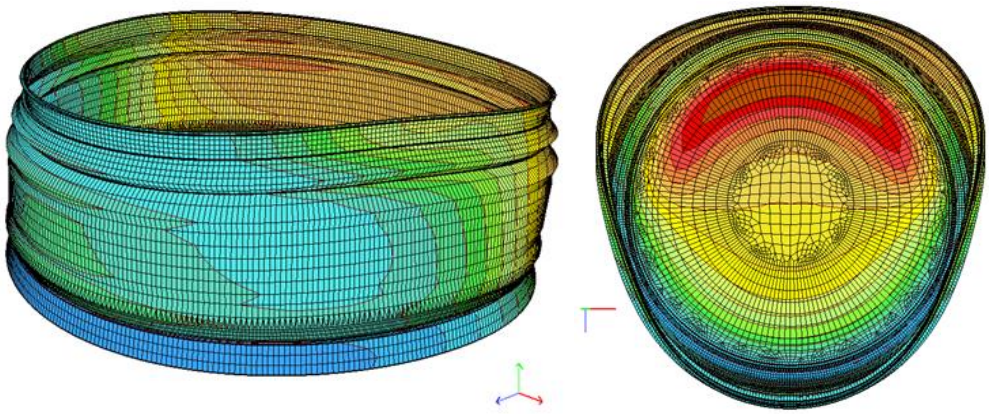

Fig. 6. The map of nodal deflections due to weakening of KZ2 and KZ3 regions, 80% with regard to the averaged subsoil stiffness modulus

Table 7. The results - settlements, variable Young's modulus of the input data - model III

No.	Annular plate				Bottom
	u_y [m]	σ_{ya} [m]	min(u_a)	max(u_a)	u_a [m]
KZ1 -0.3	-0,0192	0,0045	-0,0282	-0,0141	-0,0843
KZ1 -0.5	-0,0198	0,0048	-0,0293	-0,0141	-0.1082
KZ1 -0.8	-0,0212	0,0058	-0,0322	-0,0141	-0.2240
KZ2 -0.3	-0,0203	0,0050	-0,0346	-0,0137	-0,0692
KZ2 -0.5	-0,0218	0,0066	-0,0419	-0,0134	-0,0693
KZ2 -0.8	-0,0267	0,0134	-0,0657	-0,0124	-0,0694
KZ2 KZ4 +0.3	-0,0175	0,0043	-0,0274	-0,0118	-0,0689
KZ2 KZ4 -0.3	-0,0219	0,0054	-0,0351	-0,0136	-0,0694

Deformations of boundary courses are substantial (Fig. 6) while the irregular sheet layout affects force and strain distribution on the other side of the tank (tab. 8). Thus, the last analytical stage specifies the impact of footing parameter change on the deflections of the stiffening ring (located at the tank top). The results are collected in Tab. 8, an additional parameter is introduced to reflect the percentage of standard deviation with regard to the mean value of a given variant. The largest variation from the mean value corresponds to weakening of a smaller part along the tank foundation perimeter (the KZ reduced almost by 50%).

Table 8. Radial deflections - model III

No.	v(mean)	σ_v [m]	v [%]
KZ1 -0.3	1.094E-05	3.879E-06	35.45%
KZ2 -0.3	4.653E-03	4.036E-03	86.75%
KZ2 -0.5	9.187E-03	8.118E-03	88.35%
KZ2/4_+0.3	1.876E-03	1.152E-03	61.43%
KZ2/4_-0.3	4.593E-03	2.801E-03	60.98%
KZ2/4_-0.5	9.174E-03	5.464E-03	59.56%
KZ2/4_-0.8	2.497E-02	1.375E-02	55.06%

KZ2/3_-0.3	4.779E-03	2.900E-03	60.69%
KZ2/3_-0.5	8.399E-03	4.861E-03	57.88%
KZ2/3_-0.8	2.388E-02	1.320E-02	55.27%

Based on the conducted tests it yields that the structure exhibits deformation due to subsoil stiffness degradation. No analyzed case makes the radial displacement reach its limit value. Thus, the stiffening rings and appropriate sheet thickness required by the standards may prevent the structure from the subsoil settlement effect in this case.

4. CONCLUSIONS

The sensitivity analysis confirms a small stiffness degradation impact of distinct sub-foundation subsoil zones to the deflection variability of the bottom midpoint and the perimeter sheet. The most elevated stiffening ring of relevant (standard) parameters properly resists the circumferential deformations caused by non-uniform settlement, subsequently, by a variate subsoil stiffness. These deformations are numerically correct, checking the deflection from the perfect tank radius curvature. Local deformations are excluded which could possibly cause locking the guides of a floating roof or failure of the measurement equipment. Note that the wind rings are linked with the disadvantageous action of wind pressure. Possible extension of conducted work by impact of non-linear geometry or other in-situ aspects may led to different conclusions. Therefore, such approach may be incorporated by the Authors in the future.

5. REFERENCES

Commend, S.; Kivell, S.; Obrzud, R.; Podleś, K.; Truty, A. Zimmermann T. 2018 *Computational Geomechanics. Getting Started with ZSOIL.PC*; V.; Rossolis Editions, Switzerland: Preverenges.

Geary, W. & Hobbs, J. 2013. *Catastrophic failure of a carbon steel storage tank due to internal corrosion*. Case Studies in Engineering Failure Analysis 1: 257–264.

Grget G., Ravnjak K., Szavits-Nossan A. 2018. Analysis of results of molasses tanks settlement testing Soils and Foundations 58, 1260–1271

Gunerathne S., Seo H., Lawson W.D., Jayawickrama P.W. 2018. Analysis of edge-to-center settlement ratio for circular storage tank foundation on elastic soil Computers and Geotechnics 102,136–147

Ignatowicz R., Hotala E. 2020. Failure of cylindrical steel storage tank due to foundation settlements. Engineering Failure Analysis 115

Magnucki, K. & Lewiński, J. & Stasiewicz, P. 2004. *Optimal sizes of a ground-based horizontal cylindrical tank under strength and stability constraints*. International Journal of Pressure Vessels and Piping 81: 913–917.

Nassernia, S., Showkati H. 2020. Experimental investigation to local settlement of steel cylindrical tanks with constant and variable thickness. Engineering Failure Analysis 118

Rasiulis, K. & Šapalas, A. & Vadlūga, R. & Samofalov, M. 2006. Stress/strain state investigations for extreme points of thin wall cylindrical tanks Journal of Constructional Steel Research 62: 1232–1237.

Truty, A. 2018. On consistent nonlinear analysis of soil-structure interaction problems. *Stud. Geotech. Mech.*.

Zimmermann, T.; Sarf, J.; Truty, A.; Podles, K. 2007. Numerics for geotechnics and structures. Recent developments in ZSoil.PC. In *Applications of Computational Mechanics in Geotechnical Engineering V*; Taylor & Francis.

Żyliński, K., Korzec, A., Winkelmann, K. Górski J. Random field model of foundations at the example of continuous footing, AIP Conf. Proc. 2239 (2020). https://doi.org/10.1063/5.0007811.

Żyliński, K.; Winkelmann, K.; Górski, J. 2021. The effect of the selection of 3-D random numerical soil models on strip foundation settlements. Appl. Sci.(11).